

Ternary complex between placental lactogen and the extracellular domain of the prolactin receptor

Patricia A. Elkins^{1,2}, Hans W. Christinger¹, Yael Sandowski³, Edna Sakal³, Arie Gertler³, Abraham M. de Vos¹ and Anthony A. Kossiakoff^{1,4}

The structure of the ternary complex between ovine placental lactogen (oPL) and the extracellular domain (ECD) of the rat prolactin receptor (rPRLR) reveals that two rPRLR ECDs bind to opposite sides of oPL with pseudo two-fold symmetry. The two oPL receptor binding sites differ significantly in their topography and electrostatic character. These binding interfaces also involve different hydrogen bonding and hydrophobic packing patterns compared to the structurally related human growth hormone (hGH)–receptor complexes. Additionally, the receptor–receptor interactions are different from those of the hGH–receptor complex. The conformational adaptability of prolactin and growth hormone receptors is evidenced by the changes in local conformations of the receptor binding loops and more global changes induced by shifts in the angular relationships between the N- and C-terminal domains, which allow the receptor to bind to the two topographically distinct sites of oPL.

Prolactin (PRL), placental lactogen (PL) and growth hormone (GH) are pituitary hormones that regulate an extensive variety of important physiological functions. While growth hormone biology generally centers around the regulation and differentiation of muscle, cartilage and bone cells, it is the PRL hormones and receptors that display a much broader spectrum of activities, ranging in diversity from their well-known effects in mammalian reproductive biology to osmoregulation in fishes and nesting behavior in birds¹. An additional set of activities is induced by post-translationally modified forms of PRL and probably reacts through a noncytokine type of receptor².

The biology of PRL and GH is integrated on many levels³; however, over the 400 million years since they diverged from a common gene parent, different regulating components have evolved that distinguish them^{4,5}. In primates, the GH receptor (GHR) is activated solely by homodimerization through its cognate hormone^{4,6}. However, PRL biology works through regulated cross reactivity; most receptors are programmed to bind three hormones, PRL, PL and GH⁷.

The endocrine activities of PRL and GH are triggered by hormone induced homodimerization of their cognate receptors, which subsequently signal through a series of phosphorylation events in the JAK-STAT signaling pathway^{8,9}. The receptors belong to the hematopoietic receptor superfamily^{10,11} and have a three-domain organization: an extracellular domain (ECD) that binds the activating ligand and confers specificity, a transmembrane polypeptide of ~25 amino acids, and a cytoplasmic portion that possesses little sequence homology among members of the family. It is the cytoplasmic domains of the aggregated receptor complex that bind one or several JAK tyrosine kinases and then transphosphorylate elements on themselves, the receptors, and associated transcription factors belonging to the STAT family⁹.

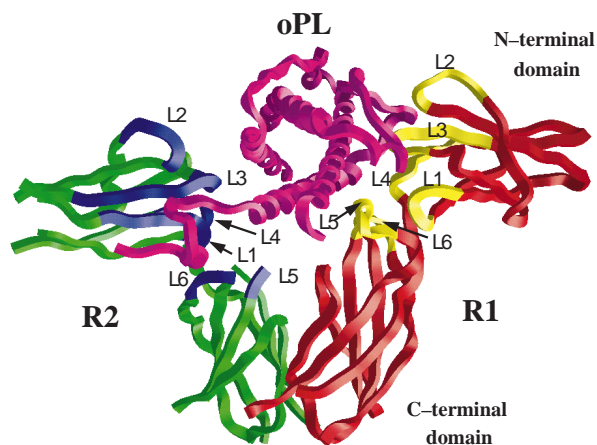


Fig. 1 The oPL–rPRLR₂ ternary complex. The binding loops on R1 and R2 are numbered. Loops L1–L3 are in the N-terminal domain of the receptor, L4 is in the linker region between the domains and L5 and L6 are in the C-terminal domain. In the R2 C-terminal domain, L5 and L6 are disordered. The β -sheet cores of the domains of R1 and R2 superimpose with an r.m.s. deviation for the N-terminal domain of 0.8 Å for 53 C α atoms; for the C-terminal domain the r.m.s. deviation is 0.5 Å for 63 C α atoms.

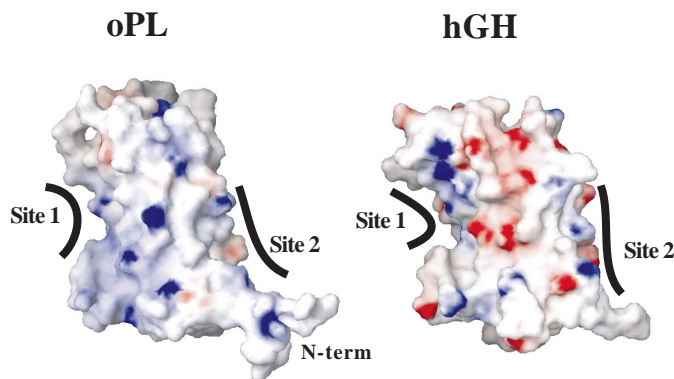
These hormones' tertiary structures play a role in how they regulate receptor activation. The structure of the ternary complex between human GH (hGH) bound to two copies of the extracellular domain (ECD) of hGHR shows that ECD1 (hGHR1) and ECD2 (hGHR2) use essentially the same set of residues to bind to two different sites on opposite faces of hGH⁶. These sites have distinctly different topographies and electrostatic character, which lead to different affinities for the receptor ECD. The high affinity site (site 1) is always occupied first by

¹Department of Protein Engineering, Genentech, Inc., 1 DNA Way, South San Francisco, California 94080, USA. ²SmithKline Beecham Pharmaceuticals, 709 Swedeland Rd., P.O. Box 1539, King of Prussia, Pennsylvania 19406-0939, USA. ³Institute of Biochemistry, Food Science and Nutrition, Faculty of Agriculture, The Hebrew University of Jerusalem, Rehovot 76100, Israel. ⁴Department of Biochemistry and Molecular Biology, The University of Chicago, Cummings Life Sciences Center, 920 E. 58th St. Chicago, Illinois 60637, USA.

Correspondence should be addressed to A.A.K. *email: koss@cummings.uchicago.edu*

articles

Fig. 4 Electrostatic rendering of hGH (left) and oPL (right). The positions of the site 1 and site 2 binding sites on each molecule are indicated by line segments. This rendering emphasizes the distinct differences in both the electrostatic and topographical character of the binding surfaces of each molecule. Electrostatic surfaces are colored between -10 kT (red) to +10 kT (blue). Molecular renderings were done using the molecular graphics program GRASP⁴⁸.



cave, while binding site 2 is an essentially flat surface. Additionally, these sites have significantly different electrostatic characters. Although about the same number of residues in both sites interact with the bound receptors, because of the differences in topography site 1 buries ~50% more surface area than site 2.

The ECDs of rPRLR are designated R1 and R2 to correspond to their association at either site 1 or site 2 of the hormone. The binding elements of R1 and R2 are a set of six surface loops numbered consecutively from L1 to L6. The extensions of these surface loops in R1 form a high affinity association in the low nM range⁵ with site 1 of oPL. In contrast, R2 cannot bind to the relatively flat surface of oPL site 2 in the absence of pre-asso-

ciated R1 at site 1. Both the N-terminal and C-terminal domains of R1 contact oPL in the complex, while only the N-terminal domain of R2 contacts the hormone (Fig. 1).

An interaction between the C-terminal domains of R1 and R2 is obligatory in forming the ternary complex. The C-terminal domains of R1 and R2 form an interface burying ~370 Å² on each receptor. The interface is asymmetric, characterized by a 10 Å shift of R1 with respect to R2 along the axis defined by the interface surface (Fig. 1).

Structure of oPL and comparison to hGH

The four-helical bundle motif of oPL (Fig. 2) is characteristic of the long chain class of cytokine hormones^{6,21,22}. The up-up, down-down four-helical bundle topology is identical to that of hGH⁶. There are three disulfide bonds in oPL: Cys (-6)–Cys 2, Cys 53–Cys 165 and Cys 182–Cys 189 (the residue numbering of oPL used here is based on that of hGH). The Cys 53–Cys 165 and Cys 182–Cys 189 disulfide bonds are conserved throughout all placental PLs, PRLs, and GHs⁴. The Cys (-6)–Cys 2 disulfide bond forms a small cyclic structure (see below) and is unique for most PRLs and placental PLs.

The aligned sequences of hGH, hPRL and oPL and a comparison of the residues involved in receptor binding for oPL and hGH are given in Fig. 3. A comparison of the hydrogen bonding interactions between each of these hormones and their respective receptors is given in Table 2. The superposition of core helical residues of oPL with hGH (taken from the hGH–hGHR₂ complex) gives a root mean square (r.m.s.) deviation of 0.8 Å for 94 C α atoms. In the nonhelical regions there are several significant differences. Due to insertions in the oPL sequence in two of the helices and subtle packing differences between the helices, the molecule is distinctly more elongated than hGH (Fig. 2). Additionally, oPL has a 12-residue N-terminal extension compared to GHs^{4,18}. Truncation of parts of this extension were shown to affect biological activity^{23,24}. This extension is structured through a short β -sheet interaction with the main body of the protein (Table 2) and contributes ~375 Å² of buried hydrophobic contact surface. The extension contains an eight-member ring formed by a disulfide bond between Cys (-6) and

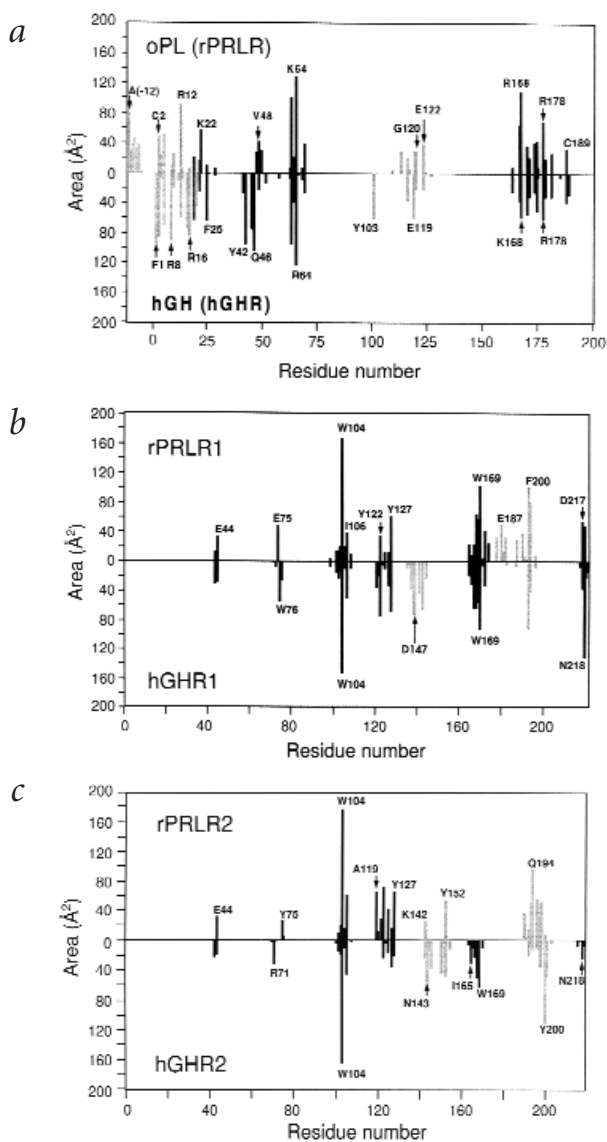


Fig. 5 Decrease in solvent accessibility on complex formation. **a**, Comparisons of hormones: oPL–rPRLR (R1 and R2) at top versus hGH–hGHR (hGHR1 and hGHR2) at bottom. Solid black lines designate site 1 contacts and gray lines represent site 2 contacts. **b**, Comparison of receptors binding at site 1; rPRLR1 (top) versus hGHR1 (bottom). **c**, Comparison of receptors binding at site 2; rPRLR2 (top) versus hGHR2 (bottom). In (b,c) the black lines designate a decrease in solvent accessibility at the hormone–receptor interface, and the gray lines designate a decrease in solvent accessibility at receptor–receptor contacts. Surface areas were calculated based on an algorithm by Lee and Richards⁴⁷.

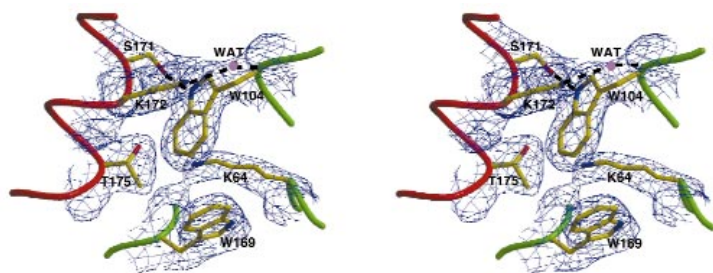


Fig. 6 A $2F_o - F_c$ Fourier map contoured at 1σ showing the packing of Trp_R 104 and Trp_R 169. A water molecule bridges between Lys 172 $\text{N}\zeta$ and Trp_R 104 O. In the hGH–hGHR₂ complex an interaction between Lys 168 $\text{N}\zeta$ and Trp_R 104 O is made directly.

Cys 2. The resulting conformation orients the side chain of Tyr (-7) into a hydrophobic cavity in R2.

Structure of the extracellular domain of rPRLR

The extracellular portion of rPRLR consists of 206 residues in two canonical fibronectin type III (FNIII) β -sheet modules (residues 31–123 and 129–245 for the N-terminal and C-terminal domains, respectively), connected by a five-residue linker (L4) that forms a single helical turn. (Residues in rPRLR are numbered based on the numbering used for hGHR⁶.) The β -sheet cores of the N-terminal and C-terminal domains of R1 and R2 in the complex have very similar structures. However, the interdomain angles between the N-terminal and C-terminal domains differ substantially, being 114° for R1 and 108° for R2. In both receptors, there is a salt bridge interaction between the two domains, from Arg_R 39 $\text{N}\epsilon$ in the N-terminal domain to Glu_R 130 $\text{O}\epsilon 1$ in the C-terminal domain (the subscript R indicates that the residues are from the receptor). The distances of this interaction are 3.0 Å and 2.9 Å for R1 and R2, respectively. Mutagenesis data suggest that this salt bridge interaction may provide stabilization of interdomain angles²⁵.

The difference in interdomain angles between R1 and R2 influences the global structure of the complex, which affects the binding footprints the receptors impart on the hormone, as well as the receptor–receptor interface between them. This is apparent when comparing its structure to those of its hGH–hGHR₂ and hGH–hPRLR1 counterparts. In the hGH–hGHR 1:2 complex⁶ the interdomain angles of both the equivalent hGHR1 and hGHR2 receptors are $\sim 90^\circ$, ~ 20 – 25° smaller than those of the rPRLR receptors in the oPL complex. These differences are primarily produced by subtle conformational changes in the six-residue domain linker, which alters the disposition of each receptor domain relative to the other. The importance of such global changes to binding specificity and regulation of activity have been suggested by several structural studies^{19,20,26–28}. For instance, the ability of hGH to cross react with both hGHR and hPRLR has been proposed to be due in part to concerted shifts in the

orientations of the receptor binding loops caused by a global change propagated by small changes in the interdomain angles of the receptor domains^{26,27}.

Comparisons of oPL and hGH binding sites

The different topographies and electrostatic characters of the site 1 and site 2 receptor binding sites of hGH and oPL are compared in Fig. 4. The buried contact surface areas for the hormone residues in sites 1 and 2 show a high degree of correspondence between oPL and hGH in their respective complexes. The buried surface area in site 1 of oPL is $\sim 985 \text{ \AA}^2$ compared to $1,250 \text{ \AA}^2$ in hGH⁶. In each case, a comparable area of the receptors is buried. Although the differences in the interdomain angles of the receptors discussed above provide an important source of conformational variation, there is little difference in the residues that are involved in the site 1 binding epitope of each hormone (Fig. 5a).

The site 1 contact epitope of the hormones includes residues on helices 1 and 4 and the C-terminal half of the crossover loop between helices 1 and 2. Most of the interactions involving helix 4 are contained within a 13-residue segment of the hormones (residues 167–179). While the residues of helix 4 that are involved in hydrogen bonds between oPL–R1, hGH–hGHR1 and hGH–hPRLR1 are generally the same, the corresponding receptor hydrogen bond partners in each of these complexes are generally not (Table 2). These structural differences appear to play a role in influencing the positioning and composition of the so-called binding ‘hot spot’²⁶. Alanine scanning mutagenesis of hGH indicates significantly different distributions of binding energy depending on which receptor hGH is bound to²⁹. Of seven hGH residues that dominate hPRLR1 binding, only two (Lys 172 and Phe 176) are also important for hGHR1 binding. One of the largest changes among the residues constituting the binding ‘hot spot’ in hGH is at position 174. The E174A hGH mutant binds to hPRLR1 1,600-fold weaker than to hGHR1³⁰, consistent with the finding that Glu 174 binds a Zn^{2+} ion, which is a required struc-

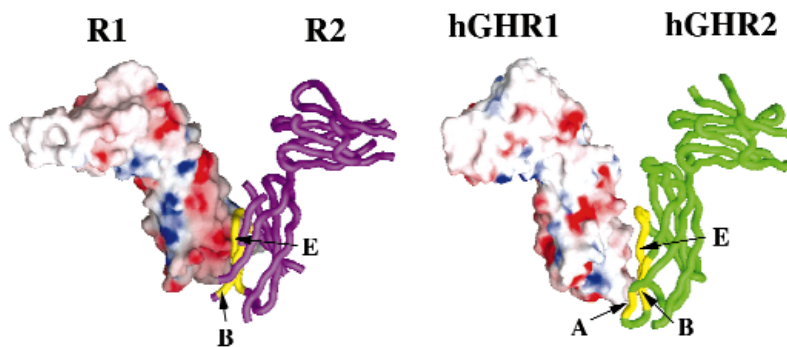
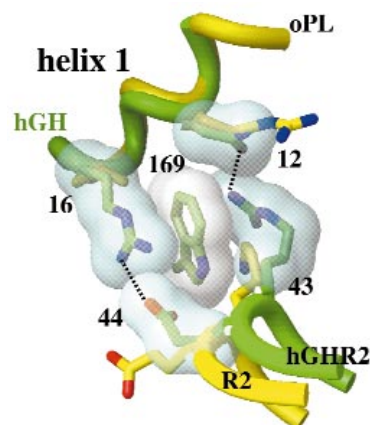


Fig. 7 Electrostatic rendering and receptor–receptor orientation for rPRLR (R1 and R2) (left) and hGHR (right). The structures were aligned by superimposing R1 and hGHR1. The alignment shows the difference in angular relationships between the two systems. The β -strands involved in the receptor–receptor contacts for R2 and hGHR2 are designated by their letters. Electrostatic surfaces are colored between -10 kT (red) to $+10 \text{ kT}$ (blue). Molecular renderings were done using the molecular graphics program GRASP⁴⁸.

articles

Fig. 8 van der Waals packing environment of Trp_R 169 at site 2 of hGH–hGHR2 superimposed onto oPL–R2. The surface rendering showing the packing of Trp_R 169 was constructed using the hGH–hGHR2 interactions. There is no similar pocket that can be formed between groups in the oPL–R2 interface.



tural feature in the hGH–hPRLR1 interface³⁰. This is not a feature of PRL or GH binding to their cognate receptors, but is apparently a specificity-dependent change that allows hGH to bind tightly to hPRLR.

In a segment of the crossover loop that connects helices 1 and 2 (residues 40–48), hGH has a two-turn helix (a so-called mini-helix) that makes substantial contact with hGHR1⁶ through two hydrogen bonds (Lys 41 N ζ to Glu_R 127 O ϵ 2 and Gln 46 N ϵ 2 to Glu_R 120 O ϵ 2). This region is disordered in oPL and, based on sequence homologies, a similar interaction is not possible between it and R1. At these two positions the hGH residues are Lys and Gln and the oPL residues are Gly and Ser; the other residues between positions 40–50 also share little sequence similarity between hGH and oPL. Additionally, the corresponding receptor residues in rPRLR are Pro_R 127 and Tyr_R 120.

Receptor elements for site 1 binding in both the oPL and hGH complexes are dominated by a network of related, but not identical, interactions. These principally involve residues Trp_R 104 on loop L3 and Trp_R 169 on loop L5 of the receptors interacting with components of helix 4 and the crossover loop between helices 1 and 2 of the hormones. This Trp_R 104/Trp_R 169 receptor ‘hot spot’³¹ has a homolog in the EPO–EPOR site 1 interface where Phe 93 and Met 150 of EPOR are direct counterparts that form a

focused hydrophobic epitope¹⁹. The packing environments for the two Trp residues in oPL–R1 are shown in Fig. 6. In both the hGH–hGHR1 and hGH–hPRLR1 structures, helix 4 is linked to Trp_R 104 through a hydrogen bond between Lys 168 N ζ and the carbonyl oxygen of Trp_R 104. Interestingly, mutagenesis data indicate that this linkage provides more binding energy in the hGH–hPRLR1 complex than in the hGH–hGHR1 complex²⁹. A somewhat different linkage exists in the oPL complex in which Ser171 O γ makes a hydrogen bond with the side chain N ϵ 1 of Trp_R 104.

For both oPL and hGH, the site 2 binding epitope involves residues in helices 1 and 3. Upon binding, ~650 Å² of the oPL surface becomes buried in the interface with R2. This compares to the ~860 Å² buried in the equivalent hGH–hGHR2 interface⁶. The oPL–R2 interface contains nine intermolecular hydrogen bonds, while that of hGH–hGHR2 contains only four (Table 2). Site 2 interactions involving the N-terminus of oPL are specific to the oPL–R2 interface (see above). Three unique hydrogen bonds bring together a region comprising residues 118–127 of the N-terminal and C-terminal domain linker region of R2 and the N-terminal segment and helix 1 of oPL (Table 3). Asp_R 124 forms a pair of hydrogen bonds, one to Tyr (-7) O η and a second to Arg 12 N η in helix 1. Arg 12 provides a second linkage to R2 through a hydrogen bond to Ile_R 103 O. The hydrogen bond network has another point of attachment between Val 116 O and Trp_R 104 N ϵ 1. Although this hydrogen bond is unique to oPL–R2, the identity and positioning of the side chains of the hydrophobic residues defining the van der Waals packing environment of Trp_R 104 are highly conserved in both complexes.

Comparison of receptor–receptor interactions

A conserved structural element of the ligand induced homodimerization of PRLRs and GHRs is a set of extensive contacts between their C-terminal domains. This receptor–receptor interface was described in detail for the hGH–hGHR₂ complex^{6,27} and modeled for the hGH–hPRLR₂ complex²⁷. Although the topology of the C-terminal domains of the rPRLRs is virtually identical to that of the C-terminal domain of the hGHRs, the receptor–receptor interfaces in these two complexes show a marked variation in their orientation and electrostatic character (Fig. 7). Also, different portions of the receptors are involved in the interaction (Fig. 5*b,c*). The surface area buried in the interaction between the rPRLRs is smaller than that buried between the hGHRs (~370 Å² compared to ~470 Å², respectively).

Eleven residues are involved in the contact interface on each rPRLR while 13 and 17 residues from hGHR1 and hGHR2,

Table 1 Composition of the final model and refinement statistics

Total number of residues	551
Number of molecules in the asymmetric unit	1
Number of water molecules ¹	136
Missing residues	
Hormone	45–47, 99–102, 191
R1	143–148
R2	55–59, 103–105, 143–149, 161–170, 180–184
Average B-factors (Å ²)	
Hormone	40
R1 (N-terminal / C-terminal domains)	37 / 46
R2 (N-terminal / C-terminal domains)	45 / 60
Completeness of data (%)	90.7
Number of unique reflections	30,300
Resolution (Å)	20–2.3
R-value (%)	23.2
R _{free} (%)	30.2
R.m.s. deviations ²	
Bonds (Å)	0.015
Angles (°)	1.7
Bond B restraints (Å ²)	2.6
Angle B restraints (Å ²)	4.4

¹Of the 136 water molecules included in the model, 50 are associated with the hormone, 61 with R1, and 25 with R2.

²For nonglycine residues 86.3% and 13.7% were in the most favored and the allowed regions in the Ramachandran plot. Four water molecules are involved in through water hydrogen bonds between hormone and receptor residues. B-factors for the water molecules average 48 Å² and range between 21 Å² and 85 Å².

Table 2 Hydrogen bonding interactions between hormones and receptors^{1,2}

Site 1					
oPL	R1	hGH	hGHR1	hGH	hPRLR1
K22N ζ	E173O ϵ 2	K41N ζ	E127O ϵ 2	S51O γ	E75O ϵ 2
N62O	I103N	P61O	I103N	S62O	M103N
K64N ζ	D164O δ 2	Q46N ϵ 2	E120O ϵ 2	Y164O η	E75O ϵ 1
R168N η 2	E75O ϵ 2	R167N δ 1	E127O ϵ 1	R167N η 1	D124O δ 2
S171O γ	W104N ϵ 1	D171O δ 2	R43N η 2	D171O δ 2	Y127O η
Y174O η	H193N ϵ 2	K168N ζ	W104O	K168N ζ	W104O
Y174O η	T171O γ 1	R178N η 2	I165O	R178N η 1	T171O γ 1
R178N η 1	G168O	T175O γ 1	R43N η 1	R178N η 2	Q193O ϵ 2
R178N η 1	W169O			R178N η 2	P170O
Site 2					
oPL	R2	hGH	hGHR2		
A(-12)N	P120O				
Q(-11)O	Y122N				
Y(-7)O η	D124O δ 2				
R12N η 1	I103O	N12O δ 1	R43N η 2		
R12N η 1	D124O δ 1	N12N δ 2	D126O δ 2		
R12N η 1	D124O δ 2	R16N η 1	E44O ϵ 2		
V116O	W104N ϵ 1	R19N η 2	E166O ϵ 1		
K113N ζ	E18O ϵ 2				
E119O ϵ 1	S102O γ				

¹Distances <3.2 Å with correct stereochemistry are considered hydrogen bonds.

²No structural information is available for hGH–hPRLR2 binding.

respectively, make up their receptor–receptor interface. The rPRLR receptor interface includes four hydrogen bonding interactions compared to six hydrogen bonding or salt bridging interactions found between hGHRs (Table 3). Although residue 201 in the first receptor hydrogen bonds across the interface in each complex, these interactions are not equivalent because of the differences in orientations of the domains.

The interactions between hGHR1 and hGHR2 generally involve the same residues on each receptor^{6,27}. In the oPL–rPRLR complex, about one third of the interface residues in R1 are also in the interface on R2. Only residues 200–201 are found in the interface for both R1 and hGHR1 (Fig. 5b). For R2, six residues from 142–154 are in the interface on hGHR2, while only residues 142 and 152 of PRLR2 are in the interface (Fig. 5c). Several residues between positions 190–200 on R2 form part of the interface for both receptors.

Implications of transient receptor dimerization

Functional and structural information suggest that the role of receptor homodimerization is more complicated than simply bringing the cytoplasmic elements of the receptors together. For instance, structural studies of EPO and EPOR indicate that a function of the hormone is to establish a fairly exact receptor alignment, as well as to induce dimerization^{28,32–34}. Based on patterns of cross-hormone and cross-species activities and the known structural differences in the active complexes, exact receptor orientation is probably not as crucial for PRL and GH systems.

Although strict orientation effects may not be crucial, it appears that the dynamics governing the stability of the aggregated signaling complex are an important regulatory element for the PRLs. Consequently, the ‘inefficient’ binding at site 2 is likely an evolved characteristic of homologous PRL systems, which distinguishes their homodimerization process from those of GH and EPO. To explain the influence of mutants on binding at site 2, a

‘minimal time’ mechanism has been proposed³⁵. This mechanism is based on the assumption that signal transduction requires a minimal persistent lifetime for the homodimer to facilitate effective transphosphorylation of the associated JAK2 kinases. Once this goal is achieved, the continued existence of the dimeric receptor complex is no longer obligatory. It is proposed that this minimal time is generally shorter for PRLRs than for GHRs, perhaps because the JAK2 kinase is preassociated with the PRLRs³⁶ but is not with GHRs³⁷. The minimal time hypothesis is also supported by a study by Pearce *et al.*³⁸, who engineered tighter and weaker binding interactions between hGH and hGHR. They found that increasing the affinities of the hGH–hGHR associations at both site 1 and site 2 produced no measurable increases in biological activity. However, reducing the affinity at site 1 by 30-fold marked a point that appeared to correspond to a threshold below which activity was affected, suggesting that wild type hGH–hGHR affinity is higher at site 1 than it needs to be to sustain full biological activity.

Structural basis for transient dimerization

The structure of the oPL–rPRLR₂ ternary complex provides some insight into the structural basis for the 1:1 rather than the 1:2 stoichiometry generally seen in PRL-like complexes. A clear difference between the oPL and hGH complexes is the relatively smaller contact surface areas of the former between the hormone and receptor 2 and at the inter-receptor interface. The inter-receptor contact areas in hGHR are ~30% larger compared to those in rPRLR and include six hydrogen bonds, compared to four between the rPRLRs. We note, however, that the inter-receptor contact surface area between EPORs¹⁹ is less than it is between rPRLRs. In fact, in a study using a small cyclic peptide to dimerize EPOR, the contact surface area was 50% smaller than that in the R1–R2 interface²⁰.

A more likely reason for the reduced binding efficiency of R2 to oPL is the absence of certain interactions with Trp_R 169, which are a major contributor to the buried hydrophobic surface area in the hGH–hGHR2 interface (Fig. 5c). Helix 1 of hGH is involved in a set of hydrogen bonding contacts to hGHR2 that are not conserved in oPL–R2 (Fig. 8). The effect of these interactions is to form a pocket into which the Trp_R 169 side chain packs tightly. In hGH, the Asn 12 side chain forms two hydrogen bonds, one through its O δ 1 to Arg_R 43 N η 2, and one through its N δ 2 with Asp_R 126 O δ 2, which is in the linker region between the N-terminal and C-terminal domains. Additionally, Arg 16 N η 1 forms a salt bridge to the carboxylate of Glu_R 44 in the N-terminal domain of hGHR2 and Arg 19 hydrogen bonds to the O ϵ 1 of Gln_R 166 in the C-terminal domain of hGHR2. The interactions involving Asn 12 and Arg 16 bracket the Trp_R 169 side chain, providing an extensive van der Waals contact surface (Fig. 8).

In oPL, Arg 12 hydrogen bonds to Asp_R 124, orienting it away from the site, and the position of Val 16 leaves the modeled Trp_R 169 side chain solvent accessible. Thus, the local environment in oPL–R2 is not conducive to productive packing of the Trp side chain (Fig. 8). We note that although the absence of a binding pocket for Trp_R 169 in oPL rationalizes the greater stability of dimeric PRL–PRLR complexes compared to ternary PRL–PRLR₂ complexes, it does not explain why hGH, which has a potential pocket, does not bind hPRLR in a 1:2 stoichiometry. Kossiakoff *et al.*²⁷ suggest that this is influenced by the stereochemical requirements of the receptor–receptor contacts. Based on the

Table 3 Receptor–receptor hydrogen bonding interactions¹

R1	R2	hGHR1	hGHR2
I188O	Q196Nε2	S145Oγ	D152Oδ2
Y200N	Q194Oε1	L146N	S201Oγ
D201Oδ1	K198N	T147Oγ	D152Oδ1
E187Oε2	K198Nζ	H150Nε2	N143Oδ1
		D152Oδ2	Y200Oη
		S201Oγ	Y200Oη

¹Distances <3.2 Å with proper stereochemistry are considered hydrogen bonds.

crystal structure of the 1:1 hGH–hPRLR complex²⁶, a set of receptor–receptor contacts were proposed²⁷ that are different from those observed in the PRL and GH complexes. In the proposed receptor orientations, the Trp_R 169 side chain is placed in a position where it has to interact with a less complementary part of the hormone interface.

What cannot be explained is the structural basis for why cross-species 1:2 complexes are more stable than their homologous species counterparts. Generally it is the case that interactions among molecules from different species result in weaker complexes. While there are cases where cross-species interactions are tighter, very rarely does this occur in such a systematic fashion as is observed in the PRL complexes. This suggests that within this family the receptors have an inherent plasticity that allows them to proficiently bind to sites that they have not been specifically optimized for. Additionally, it appears that the evolutionary development of a weaker binding interaction at site 2 within species is actually an optimization strategy, presumably to fine-tune the regulation of the receptor's activity.

Methods

Protein purification, complex formation and crystallization.

oPL and rPRLR were purified as described^{13,15}. Briefly, both proteins were expressed in *Escherichia coli* cells and extracted from inclusion bodies. After refolding, they were purified by anion exchange chromatography (Q-Sepharose column, Pharmacia) and lyophilized. oPL and rPRLR were solubilized in buffer at pH 7.5 and mixed together in a 1:2.1 molar ratio. The oPL–rPRLR₂ complex was purified by size exclusion chromatography and stored at 4 °C for crystallization experiments. Detailed crystallization and data collection have been described³⁹.

Crystal data. Monoclinic crystals of the complex grew in space group C2 with unit cell parameters $a = 168.2$ Å, $b = 63.1$ Å, $c = 88.4$ Å, $\beta = 118.6^\circ$ and one complex in the asymmetric unit. Crystals contained isopropanol (15%) as a cryoprotectant and crystal manipulations were done in a glove box that was saturated with isopropanol to prevent crystal damage. An initial data set was corrupted by an ice ring that systematically masked reflections in a shell between 3.9–3.4 Å resolution. The problem was circumvented in subsequent data sets by eliminating a viscous film that formed on the surface of the sitting drops. This approach greatly improved the success of the flash freezing process. A crystal prepared in this manner produced a complete data set to 2.3 Å resolution collected at the Cornell High Energy Synchrotron Source (CHESS; overall completeness to 2.3 Å was 91% with an R_{merge} of 6.0%). These data had an $I / \sigma I$ of 16.2 for all data and 4.6 for the last shell of data (2.4–2.3 Å). Data to 2.7 Å resolution were also collected at CHESS from a frozen crystal of a potential mercury derivative (overall completeness to 2.65 Å was 97% with an R_{merge} of 4.1%).

oPL–R1–R2 structure solution. The structure was solved by molecular replacement using the software package AmoRE⁴⁰. The oPL

and R1 were unambiguously placed in the unit cell by rotation and translation function calculations (R-value and correlation coefficients of 52% and 0.29, respectively) using the crystal structure of the 1:1 complex of hGH–hPRLR¹²⁶ as a model. There was no apparent rotation solution for R2 using the structure of a single hPRLR as a model. Based on the assumption that the interaction of R2 with oPL would be similar to the interactions hGHR makes with hGH, a template model of a 1:1 complex of hGH with a hPRLR interacting at site 2 was prepared by superimposing the structure of R2 onto hGHR2 in the 1:2 hGH–hGHR complex. Although there was no definitive rotation solution for the modeled complex, a rotation solution was chosen that best fit the criteria that oPL would have the same orientation in the unit cell as had been determined from the earlier calculations for the 1:1 complex. In an iterative fashion, a translation function was calculated for each individual protein in the complex while fixing the remaining two proteins. Rigid body refinement led to an R-value of 51.7% and an R_{free} of 52.2%, obtained for the range 10–3 Å.

Throughout the early stages of refinement, the electron density for R2 was of poorer overall quality and ambiguous in the C-terminal domain. This suggested that R2 might be misplaced relative to oPL and R1. To reorient the C-terminal domain of R2, a modified rotation function with Patterson correlation (PC) refinement was run in X-PLOR⁴¹ based on the C-terminal domain of hPRLR. The F_o data used in the rotation function were modified by subtracting from the experimentally measured F_o the F_c corresponding to the correctly oriented portion of the complex, that is, all parts of the complex except the C-terminal domain of R2^{42,43}. Such a procedure significantly improved the signal-to-noise ratio in the function and allowed for a reliable placement of the C-terminal domain of R2.

Model refinement. The model was refined with X-PLOR⁴¹ using noncrystallographic symmetry restraints for the β -sheet portions of the two receptors. Maps were calculated with CCP4⁴⁰ using SIGMAA weighting, and manual rebuilding was done using O⁴⁴.

Data from 20.0–2.3 Å resolution were included in the refinement and a random set of 2,039 reflections were set aside for the calculation of R_{free} ⁴⁵. Individual temperature factors were calculated, and a bulk solvent correction ($k = 0.26e / \text{Å}^3$, $B = 67 \text{ Å}^2$) to the data was added. Cycles of refinement in the program REFMAC⁴⁰ were alternated with cycles of refinement in X-PLOR. Solvent molecules were selected using the WATERPICK facility in QUANTA to fit 4 σ peaks in the SIGMAA⁴⁶ weighted $F_o - F_c$ map. All solvent molecules were required to have temperature factors less than 85 Å² and density in the 2 $F_o - F_c$ electron density map of at least 1 σ .

Model bias. Even with the corrected placement of the C-terminal domain of R2, pervasive problems with model bias existed, which impeded the refinement process. The model bias was reduced by inclusion of experimental phase information using cross-crystal averaging from a nonisomorphous mercury derivative. The unit cell of a crystal soaked in methyl mercury iodide differed from that of the native by 2.1% on the b axis and by 3.3% on the c axis. The R_{iso} between these data and the native was 0.37. In cross-crystal averaging using the program DM⁴⁰, the derivatized crystal could be considered a second crystal form. Averaging improved the maps significantly, and, from this point, the refinement of the model progressed smoothly. The surface area buried on complex formation was calculated with programs from the CCP4 suite⁴⁰.

Coordinates. The coordinates have been deposited in the Protein Data Bank (accession code 1F6F).

Acknowledgments

We thank the staff at the SSRL and at CHESS for help with beamlines 7-1 and A-1, respectively; M. Randal, C. Eigenbrot, N. Gerber, Y. Muller and C. Wiesmann for help with data collection; and W. Anstine and B. Bernat for help with the figures. Part of this research was supported by the United States–Israel Binational Science Foundation.

Received 9 March, 2000; accepted 26 July, 2000.

1. DeVlaming, V. Actions of prolactin among the vertebrates. In *Hormones and evolution* (ed., Barrington, E.J.W.), 561–642 (Academic Press, New York; 1979).
2. Sinha, Y.N. Structural variants of prolactin: occurrence and physiological significance. *Endocrine Rev.* **16**, 354–369 (1995).
3. Goffin, V., Shiverick, K.T., Kelly, P.A. & Martial, J.A. Sequence-function relationships within the expanding family of prolactin, growth hormone, placental lactogen, and related proteins in mammals. *Endocrine Rev.* **17**, 385–410 (1996).
4. Nicoll, C.S., Mayer, G.L. & Russel, S.M. Structural features of prolactins and growth hormones that can be related to their biological properties. *Endocrine Rev.* **7**, 169–203 (1986).
5. Gertler, A., Grosclaude, J., Strasburger, C.J., Nir, S. & Djiane, J. Real-time kinetic measurements of the interactions between lactogenic hormones and prolactin-receptor extracellular domains from several species support the model of hormone-induced transient receptor dimerization. *J. Biol. Chem.* **271**, 24482–24491 (1996).
6. De Vos, A.M., Ultsch, M. & Kossiakoff, A.A. Human growth hormone and extracellular domain of its receptor: crystal structure of the complex. *Science* **255**, 306–312 (1992).
7. Kelly, P.A., et al. The growth hormone/prolactin receptor gene family. *Oxford Surveys On Eukaryotic Genes* **7**, 29–50 (1991).
8. Schindler, C. & Darnell, J.E.J. Transcriptional responses to polypeptide ligands: the JAK-STAT pathway. *Annu. Rev. Biochem.* **64**, 621–651 (1995).
9. Ihle, J.N., et al. Signaling by the cytokine receptor superfamily: JAKs and STATs. *Trends Biochem. Sci.* **19**, 222–227 (1994).
10. Bazan, J.F. Structural design and molecular evolution of a cytokine receptor superfamily. *Proc. Natl. Acad. Sci. USA* **87**, 6934–6938 (1990).
11. Cosman, D., et al. A new cytokine receptor superfamily. *Trends Biochem. Sci.* **15**, 265–270 (1990).
12. Fuh, G., et al. Rational design of potent antagonists to the human growth hormone receptor. *Science* **256**, 1677–1680 (1992).
13. Sandowski, Y., et al. Preparation and characterization of recombinant prolactin receptor extracellular domain from rat. *Mol. Cell. Endocrinol.* **115**, 1–11 (1995).
14. Tchelet, A. Extracellular domain of prolactin receptor from bovine mammary gland: expression in *Escherichia coli*, purification and characterization of its interaction with lactogenic hormones. *J. Endocrinol.* **144**, 393–403 (1995).
15. Sakal, E., et al. Large-scale preparation and characterization of recombinant ovine placental lactogen. *J. Endocrinol.* **152**, 317–327 (1997).
16. Sakal, E., et al. Cloning, preparation, and characterization of biologically active recombinant caprine placental lactogen. *J. Endocrinol.* **159**, 509–518 (1998).
17. Sakal, E., Elberg, G. & Gertler, A. Direct evidence that lactogenic hormones induce homodimerization of membrane-anchored prolactin receptor in intact Nb2-11C rat lymphoma cells. *FEBS Lett.* **410**, 289–292 (1997).
18. Colosi, P., et al. Cloning and expression of ovine placental lactogen. *Mol. Endocrinol.* **3**, 1462–1469 (1989).
19. Syed, R.S., et al. Efficiency of signalling through cytokine receptors depends critically on receptor orientation. *Nature* **395**, 511–516 (1998).
20. Livnah, O., et al. Functional mimicry of a protein hormone by a peptide agonist: the EPO receptor complex at 2.8 Å. *Science* **273**, 464–471 (1996).
21. Kossiakoff, A.A. & De Vos, A.M. Structural basis for cytokine hormone-receptor recognition and receptor activation. *Adv. Protein Chem.* **52**, 67–108 (1998).
22. Abdel-Meguid, S.S., et al. Three-dimensional structure of a genetically engineered variant of porcine growth hormone. *Proc. Natl. Acad. Sci. USA* **84**, 6434–6437 (1987).
23. Rhee, H.K., et al. Biological activity and immunological reactivity of human prolactin mutants. *Endocrinology* **136**, 4990–4995 (1995).
24. Gertler, A., et al. Preparation, purification, and determination of the biological activities of 12 N terminus-truncated recombinant analogues of bovine placental lactogen. *J. Biol. Chem.* **267**, 12655–12659 (1992).
25. Rosakis-Adcock, M. & Kelley, P.A. Identification of ligand binding determinants of the prolactin receptor. *J. Biol. Chem.* **267**, 7428–7433 (1992).
26. Somers, W., Ultsch, M., De Vos, A.M. & Kossiakoff, A.A. The X-ray structure of the growth hormone-prolactin receptor complex. *Nature* **372**, 478–481 (1994).
27. Kossiakoff, A.A., et al. Comparison of the intermediate complexes of human growth hormone bound to the human growth hormone and prolactin receptors. *Protein Sci.* **3**, 1697–1705 (1994).
28. Wilson, I.A. & Jolliffe, L.K. The structure, organization, activation and plasticity of the erythropoietin receptor. *Curr. Opin. Struct. Biol.* **9**, 696–704 (1999).
29. Cunningham, B.C. & Wells, J.A. Rational design of receptor-specific variants of human growth hormone. *Proc. Natl. Acad. Sci. USA* **88**, 3407–3411 (1991).
30. Cunningham, B.C., Bass, S., Fuh, G. & Wells, J.A. Zinc mediation of the binding of human growth hormone to the human prolactin receptor. *Science* **250**, 1709–1712 (1990).
31. Clackson, T. & Wells, J.A. A hot spot of binding energy in a hormone-receptor interface. *Science* **267**, 383–386 (1995).
32. Remy, I., Wilson, I.A. & Michnick, S.W. Erythropoietin receptor activation by ligand-induced conformation change science. *Science* **283**, 990–993 (1999).
33. Livnah, O., et al. An antagonist peptide-EPO receptor complex suggests that receptor dimerization is not sufficient for activation. *Nature Struct. Biol.* **5**, 993–1004 (1998).
34. Livnah, O., et al. Crystallographic evidence for preformed dimers of erythropoietin receptor before ligand activation. *Science* **283**, 987–990 (1999).
35. Herman, A., Helman, D., Livnah, O. & Gertler, A. Ruminant placental lactogens act as antagonists to homologous growth hormone receptors and as agonists to human or rabbit growth hormone receptors. *J. Biol. Chem.* **274**, 7631–7639 (1999).
36. Lebrun, J.J., Ali, S., Sofer, L., Ullrich, A. & Kelly, P.A. Prolactin-induced proliferation of Nb2 cells involves tyrosine phosphorylation of the prolactin receptor and its associated tyrosine kinase JAK2. *J. Biol. Chem.* **269**, 14021–14026 (1994).
37. Argetsinger, L., et al. Identification of JAK2 as a growth hormone receptor-associated tyrosine kinase. *Cell* **74**, 237–244 (1993).
38. Pearce, K.H., Cunningham, B.C., Fuh, G., Teeri, T. & Wells, J.A. Growth hormone binding affinity for its receptor surpasses the requirements for cellular activity. *Biochemistry* **38**, 81–89 (1999).
39. Christinger, H.W., et al. Crystallization of ovine placental lactogen in a 1:2 complex with the extracellular domain of the rat prolactin receptor. *Acta Crystallogr. D* **54**, 1408–1411 (1998).
40. Collaborative Computational Project, Number 4. CCP4 Suite: programs for protein crystallography. *Acta Crystallogr. D* **50**, 760–763 (1994).
41. Brünger, A.T. X-PLOR reference manual 3.0 edn (Molecular Simulations, Inc., Waltham, Massachusetts; 1992).
42. Huang, M., et al. The mechanism of an inhibitory antibody on TF-initiated blood coagulation revealed by the crystal structures of human tissue factor, Fab 5G9 and TF.G9 complex. *J. Mol. Biol.* **275**, 873–894 (1998).
43. Zhang, X.J. & Matthews, B.W. Enhancement of the method of molecular replacement by incorporation of known structural information. *Acta Crystallogr. D* **50**, 675–686 (1994).
44. Inaka, K., Taniyama, Y., Kikuchi, M., Morikawa, K. & Matsushima, M. The crystal structure of a mutant human lysozyme C7795A with increased secretion efficiency in yeast. *J. Biol. Chem.* **266**, 12599–12603 (1991).
45. Brünger, A.T. Free R value: a novel statistical quantity for assessing the accuracy of crystal structures. *Nature* **355**, 472–475 (1992).
46. Read, R. Improved Fourier coefficients for maps using phases from partial structures with errors. *Acta Crystallogr. A* **42**, 140–149 (1986).
47. Lee, B. & Richards, F.M. The interpretation of protein structures: estimation of static accessibility. *J. Mol. Biol.* **55**, 379–400 (1971).
48. Nicholls, A., Bharadwaj, R. & Honig, B. GRASP: graphical representation and analysis of surface properties. *Biophys. J.* **64**, A166 (1993).